CONCERNING THE DAMAGE OF STAINLESS STEELS BY CAVITATION EROSION

Mădălina-Elena MÂNZÂNĂ[1], Bânduşa GHIBAN[2], Mihai MARIN[3], Nicolae GHIBAN[4], Ilare BORDEAŞU[5], Sorina MITREA[6], Florin MICULESCU[7]

Lucrarea prezintă rezultatele experimentale asupra comportamentului la eroziunea prin cavitație a diferitelor tipuri de oțeluri inoxidabile. Cercetările sunt realizate în laboratorul de cavitație al Universității Politehnica din Timişoara (LMHT), pe un aparat vibrator care respectă condițiile stabilite prin normele ASTM G32-2006. Oțelurile inoxidabile au fost cercetate pe baza analizei macrostructurale şi microscopie electronică la care s-au determinat caracteristicile structurale: zona afectată de cavitație, raportul dintre zona afectată şi zona neafectată de cavitație (prin măsurarea diametrelor). De asemenea, probele au fost analizate prin difracție de raze unde s-au identificat fazele acestora.

This paper presents the experimental results of cavitation erosion behavior of some stainless steels. The experimental investigations were performed in magnetostrictive vibrating apparatus at Cavitation Laboratory of Polytechnic University of Timisoara (LMHT) in according with ASTM G32-2006. Several investigations were done on macro structural analysis and electron microscopy where determined many structural features, such as affected area destroyed by cavitation, ratio between affected and nonaffected cavitation areas through diameter measurements. Also, the samples was analysed through X-ray diffraction where there phases were identified.

Keywords: cavitation, erosion, depth, chemical composition, stainless steel

[1] PhD Student, Depart. of Materials Science and Engineering, University POLITEHNICA of Bucharest, Romania, e-mail: madalina_manzana@yahoo.com
[2] Prof., Depart. of Materials Science and Engineering, University POLITEHNICA of Bucharest, Romania
[3] Prof., Depart. of Materials Science and Engineering, University POLITEHNICA of Bucharest, Romania
[4] Prof., Depart. of Materials Science and Engineering, University POLITEHNICA of Bucharest, Romania
[5] Prof., Depart. of Materials Hydraulic Machines, University "Timisoara" of Bucharest, Romania
[6] Eng., National Institute for Research and Development in Electrical Engineering, România
[7] Lecturer, Depart. of Materials Science and Engineering, University POLITEHNICA of Bucharest, Romania

1. Introduction

The search for the origin of erosion by cavitation bubbles is nearly one hundred years old: it was initiated by the finding of severe destructive effects on the propellers of the great ocean liners Lusitania and Mauretania, reported first by Silberrad (1912). This was the beginning of investigations of bubble dynamics by numerous researchers all over the world [1].

While the history of cavitation has been traced back to the middle of the eighteenth century, little reference to cavitation pertaining directly to the marine industry has been found until the mid-nineteenth century [2].

Cavitation erosion is a common cause of failure in machinery such as hydro-turbines, ship propellers, pumps, valves, diesel engines and is a important factor in many areas of science, engineering, including acoustics, chemistry and metallurgical [3, 4,5,6,7].

Cavitation is a general fluid mechanics phenomenon that can occur whenever a liquid is used in a machine which induces pressure and velocity fluctuations in the fluid [8]. Pressure differentials in the fluid generate gas or vapor bubbles in the fluid. When these bubbles encounter a high-pressure zone, they collapse and cause explosive shocks to the surface. These surface shocks cause localized deformation and pitting. Cavitation pits eventually link up and cause a general roughening of the surface and material removal. Cavitation is similar to particle erosion in its damage [9].

Cavitation can take different forms as it develops from inception. Some authors revealed correlation between structure and properties of different metallic materials in connection with cavitation erosion resistance [10]. The aim of present paper is to put in evidence the erosion- cavitation demage of different stainless steels through structural characterization.

2. Materials and Methods of Investigations

Different stainless steels were investigated in order to reveal erosion-cavitation behaviour. The chemical composition of the experimental stainless steels made by spectrometry is given in table 1. In according with Schaeffler diagram, after determining equivalents in chromium and in nickel we consider two types of stainless steels, austenitic stainless steel (steels C and D) and austenitic – ferritic stainless steels (steels A, B, E, F, G and H) with different percents of constituents.

The cavitation erosion tests were carried out in a magnetostrictive facility, in according with Standard Test Method for Cavitation Erosion Using Vibratory Apparatus (ASTM G32), using as cavitant liquid drink water at 20 $\pm 1^0$C [11,12,13].

Table 1

Chemical composition of the experimental stainless steels

Alloy	Element ,wt.%												
	Si	**Mn**	**Mo**	**Cr**	**Ni**	**Al**	**Ti**	**P**	**S**	**Cu**	**Fe**	**E_{Cr}**	**E_{Ni}**
A	3.59	3.16	-	18.54	7.59	1.83	0.77	0.03	0.012	-	ball	23.925	11.57
B	1.91	3.45	-	21.18	8.59	2.72	1.13	0.04	0.013	-	ball	24.045	11.215
C	1.38	2.69	2.86	21.37	23.4	2.17	-	0.04	0.015	2.82	ball	26.30	24.34
D	1.81	2.56	2.64	21.30	22.19	-	-	0.04	0.013	3.48	ball	26.655	23.47
E	1.73	2.48	2.66	20.88	8.00	-	-	0.04	0.015	-	ball	26.135	10.74
F	2.18	2.10	2.47	19.31	8.17	-	-	0.04	0.015	0.86	ball	25.05	10.72
G	0.99	2.50	-	20.62	8.71	-	0.83	0.03	0.012	-	ball	22.105	11.46
H	3.87	5.38	-	19.99	11.73	1.87	-	0.04	0.012	-	ball	25.795	15.02

Cavitation erosion behaviour after 165 minutes was appreciated considering macrostructural analysis made at stereomicroscope type OLYMPUS equipped with QuickMicrophoto 2.2 software.

Also, the samples of stainless steels were cut for microscopic analysis (SEM/EDS) and for X-ray diffraction analysis. For SEM samples were examined in a scanning electron microscope type Philips XL 30 ESEM TMP equipped with secondary electron detector in low-vacuum and solid state backscattered electrons signals (BSE) detector with two diodes [14]. The XRD were made on D8 ADVANCE diffractometer with molybdenum K_α radiation because the sample has iron composition and the samples were measured in average from 10° to 90° with a step size of 0.040°, the scan step time was 1 second.

3. Results and interpretations

Results concerning structural investigation of cavitation behaviour of the investigated stainless steel are given in next figures.

Stereomacrostructural aspects of the experimental test samples are given in Fig. 1.

In steel A and steel B the surface attacked by cavitation is found approximately in a concentric circle (Fig. 1a, 1b), on may observe that macroscopic interconnected cavitations with radial disposal so this aspect gives best behavior from a macroscopic point of view.

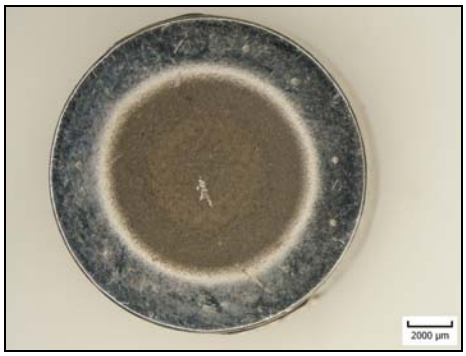

a

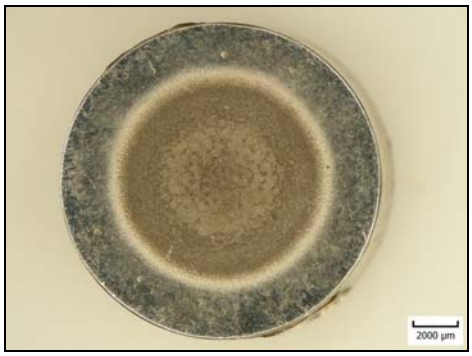

b

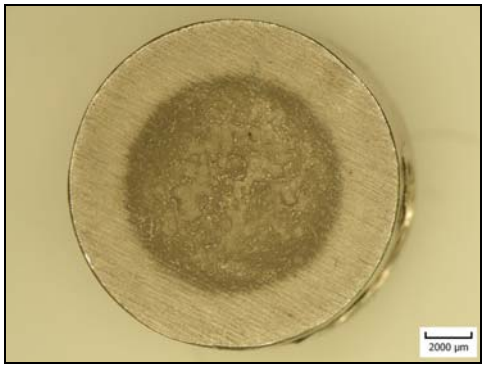

c

d

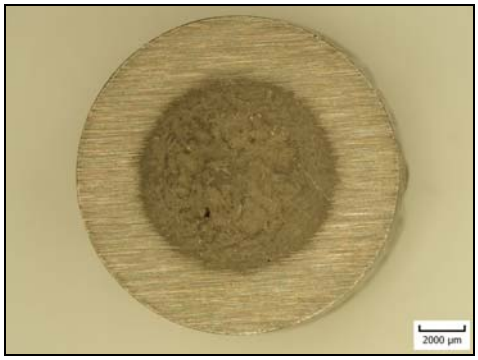

e

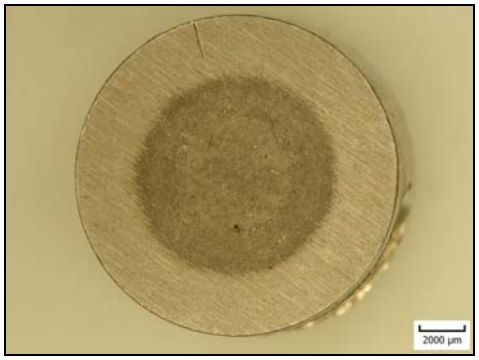

f

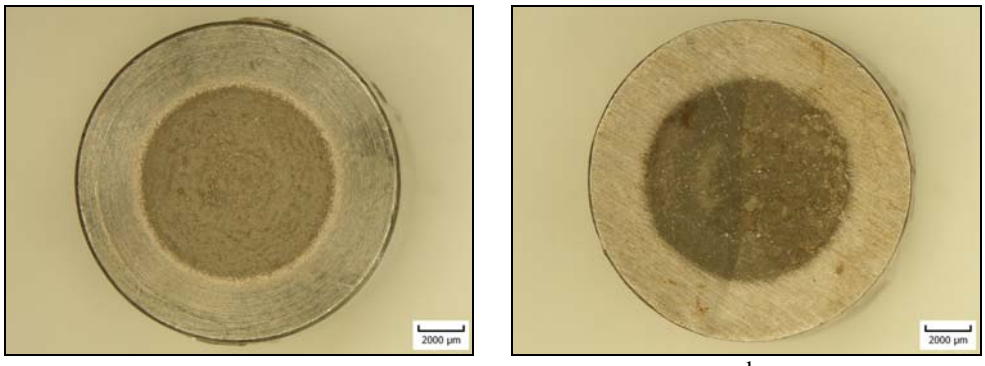

g h

Fig. 1 Stereomacroscopic aspect of experimental samples, x8:
a- steel A ; b- steel B ; c- steel C ; d- steel D ; e- steel E ; f- steel F ; g- steel G ; h- steel H

Steels C, E, F, with the behavior given in figures 1c, 1e, respectively fig. 1f, has also concentric circle aspects of the affected surfaces by cavitation. The difference from previous images consists a highly degraded surface with many interconnected cavitations and radial disposal.

In the steel D from figure 1d, with 100% austenite, the surface degraded through cavitation is well delimitated and it has huge interconnected cavitations with radial disposal.

On steel G, with 60% austenite and 40% ferrite, the surface degraded through cavitation is well delimitated and it presents many cavitations with uniform disposal (Fig. 1g). At, steel H from figure 1h, with 80% austenite and 20% ferrite, the cavitation attack is also found approximately in a concentric circle, many cavitations with non-uniform disposal and the right side is more affected by corrosion than the left.

The extension of cavitation phenomenon is given in figure 2 and table 2, which may give the possibility of making a comparison concerning cavitations behaviour.

Tabel 2

Different measurements for investigated different stainless steels after cavitation

Alloy	Sample diameter, µm	Extension of cavitation, µm	Surface affected by cavitation, %	Depth of cavitation, µm
A	13736	8780	41	305
B	13749	8733	40	275
C	13836	9162	44	540
D	13654	8866	42	325
E	13718	8456	38	515
F	13738	8554	39	326
G	13560	8374	38	335
H	13765	8762	41	400

So at steel A only 40.86% surface is affected by cavitation (Fig. 2a), about 40.35% of surface is affected by cavitation in steel B (Fig. 2b). The highest affected surface by cavitation is met at austenite stainless steel C, where 43.85 % of surface is affected by cavitation (Fig. 2c) and well defined cavitations are about 300-400μm diameters.

In steel D a surface about 42.16 % of is affected by cavitation (Fig. 2 d), about 38 % of surface is affected by cavitation in steel E (Fig. 2e), and, respectively about 38.77 % of surface is affected by cavitation in steel F (Fig. 2f) but the real affected cavitation surface can be smaller, due to very deep frame cavitations. At steel G only 38.14 % surface is affected by cavitation (Fig. 2g) where all the cavitations are uniform distributed inside the affected surface, and at steel H a surface about 40.52% is affected by cavitations (figure 2h), where one may remark also a general corrosion of surface. The best cavitation behaviour is for stainless steel with 20% austenite and 80% ferrite (steel E).

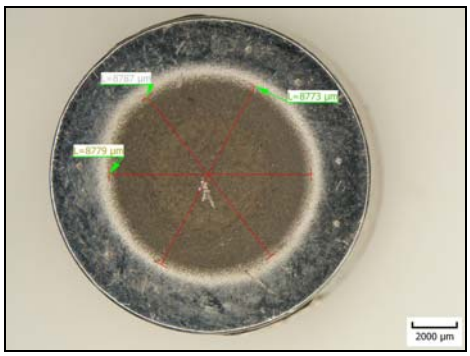

a

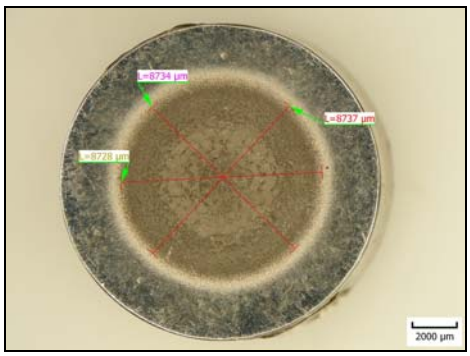

b

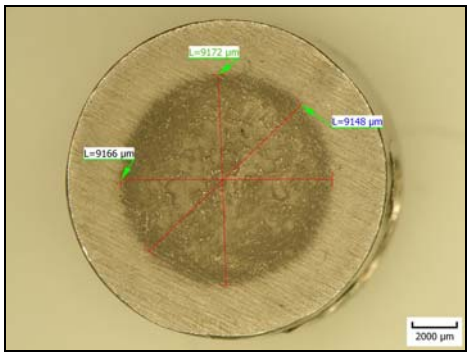

c

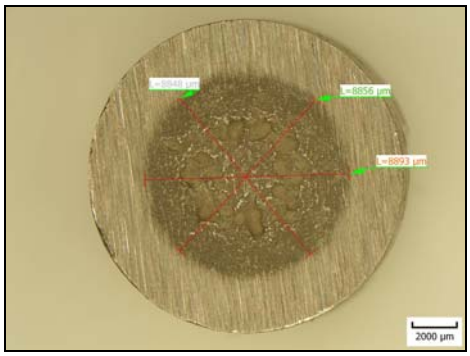

d

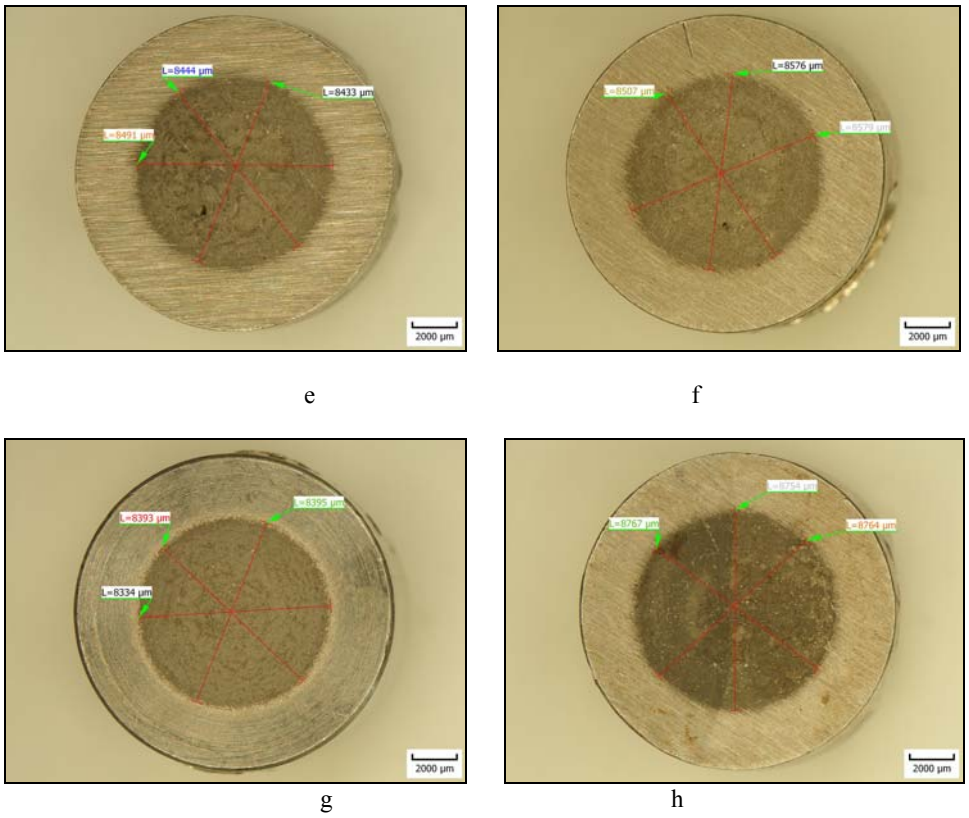

Fig. 2 Stereomacrostructural aspect of samples after
measuring cavitation affected zone, x8
a- steel A ; b- steel B ; c- steel C ; d- steel D ; e- steel E ; f- steel F ; g- steel G ; h- steel H

Fig. 3 indicates the depths of the erosion cavity in the investigated samples. The depth of erosion cavity is in the range of 300-540µm for the investigated stainless steels. The highest value of depth is met in case of steel C, with about 540µm (Fig. 3c), followed by steel E with about 515µm (Fig. 3e), in comparison with the other, where the depth is 305µm for steel A (Fig. 3a), 275µm for steel B (Fig. 3b), 325µm for steel D (Fig. 3d), 326µm for steel F (Fig. 3f), 335 µm for steel G (Fig. 3g) and, respectively 400µm for steel H (Fig. 3h).

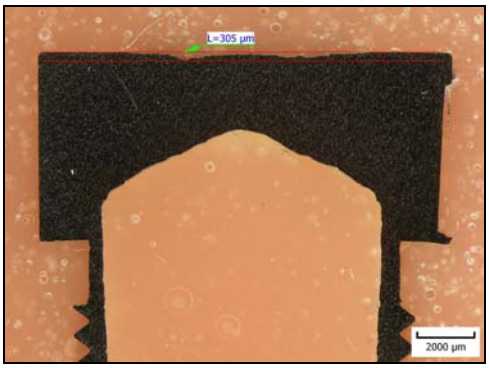
L=305 µm
2000 µm

a

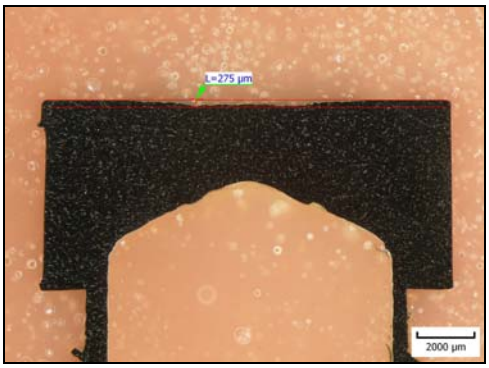
L=275 µm
2000 µm

b

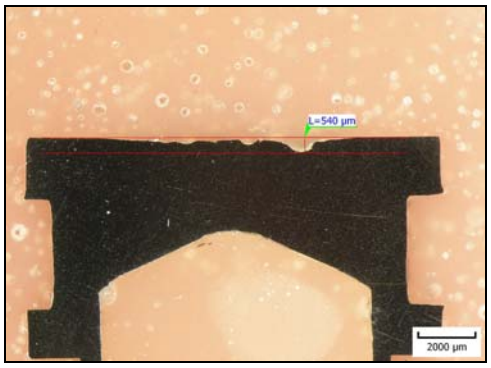
L=540 µm
2000 µm

c

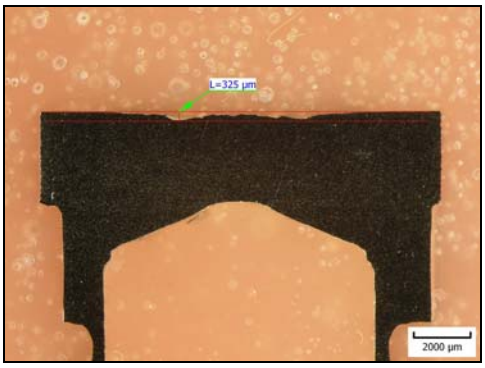
L=325 µm
2000 µm

d

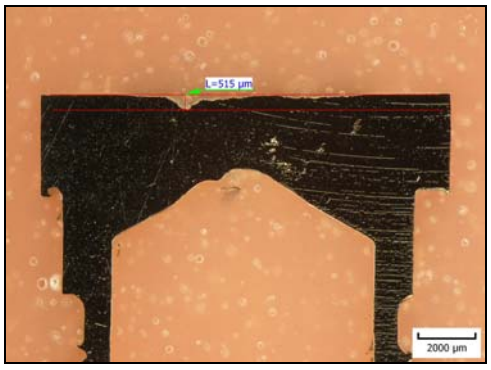
L=515 µm
2000 µm

e

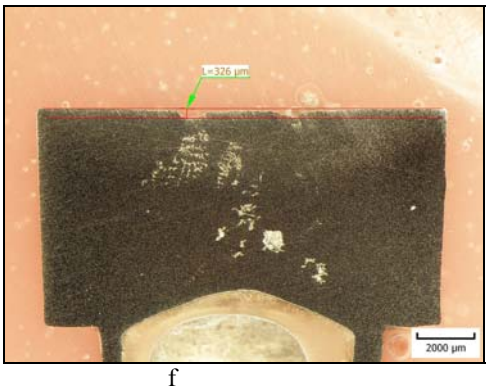
L=326 µm
2000 µm

f

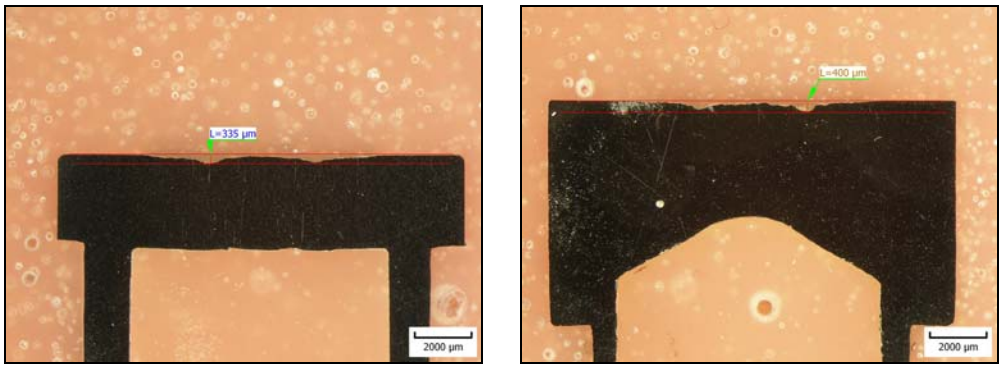

g h

Fig. 3. Tranversal cross sections of erosion cavitation samples:
a-steel A (with 305µm depth); b- steel B (with 275µm depth); c- steel C (with 540µm depth); d-steel D (with 325µm depth); e- steel E (with 515µm depth); f- steel F (with 326µm depth); g- steel G (with 335µm depth); h- steel H (with 400µm depth)

Fig. 4 reveals the structural analysis at scanning electron microscope of the experimental stainless steels. So, at steel A is observed surface with very fine cavitations; aspect mixed of cavitations; fragile character breaking with propagation intergranular and cracks cleavage planes (Fig. 4a). At steel B, is observed surface with fine cavitations and many cavity uniform degradation with fine and intergranulation very fine cracks and dimensions of cavitations about 10-15µm; fragile breaking with aspect intergranular with highlight a cavity of 5 µm and sliding paths (Fig. 4b). At steel C (Fig. 4c) one may reveal equal proportions of fine and big cavitations; the surface with deep secondary intergranular cracks; fragile character breaking with intergranular propagation and sliding paths. At steel D, reveals that aspect mixed of cavitations, with fine and big cavitations, surfaces with deep secondary intergranular cracks and many cavity uniform disposal; fragile breaking aspect with intergranular propagation and plane of cleavage (Fig. 4d).

In steel E, (Fig. 4e) the eroded surface presents a mixed aspect of cavitations, surface with very fine cavity initiated by nonmetallic inclusions; brittle fracture with very fine intergranular cracks, cleavage planes and propagation of wave breaking front. At steel F, the surface is with very fine cavitations and fine intergranular cracks; aspect mixed of cavitations with cleavage planes, propagation of the front by very fine intergranular cracks and cleavage planes (Fig. 4f).

On steel G, there are put in evidence (Fig. 4g) surface with equal proportions of fine and big cavitations, the surface with secondary intergranular cracks, propagations through cleavage with accentuate sliding plane; fragile character breaking with intergranular propagation. At steel H, the eroded surface presents a mixed surface; intergranular and transcrystalline propagation; fragile

character breaking with intergranular aspect and cavitations with intergranular cracks (Fig. 4h).

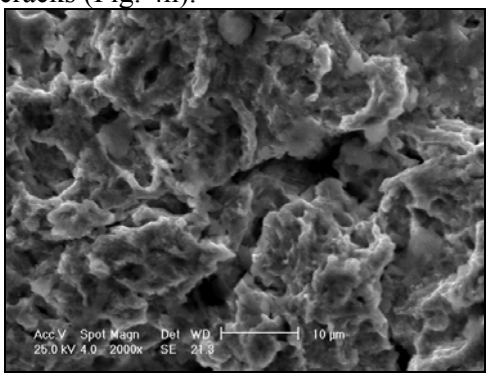

a

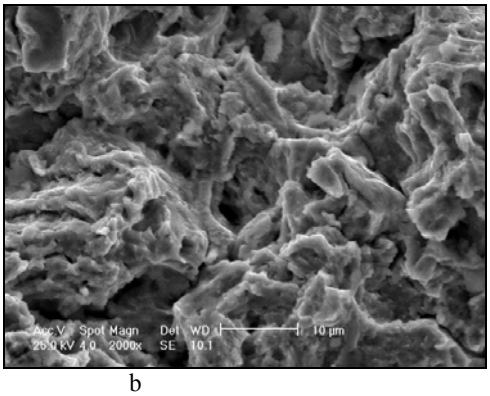

b

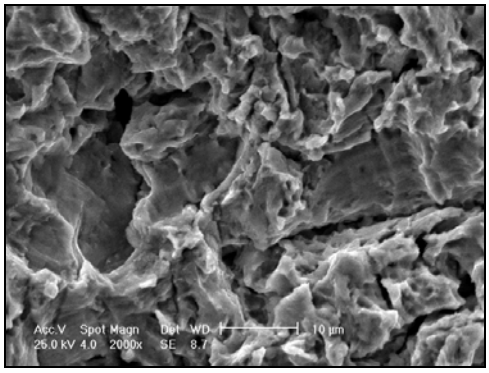

c

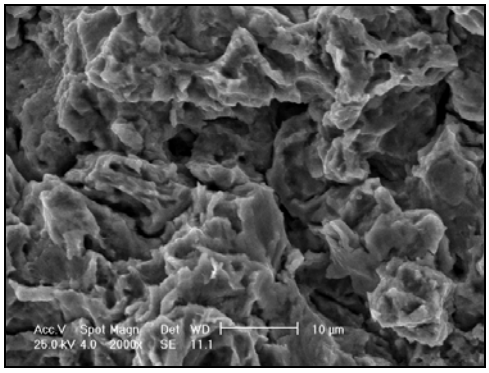

d

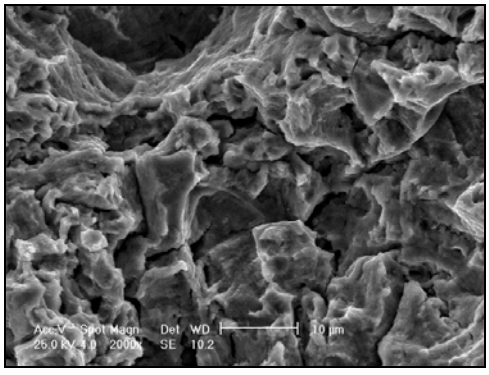

e

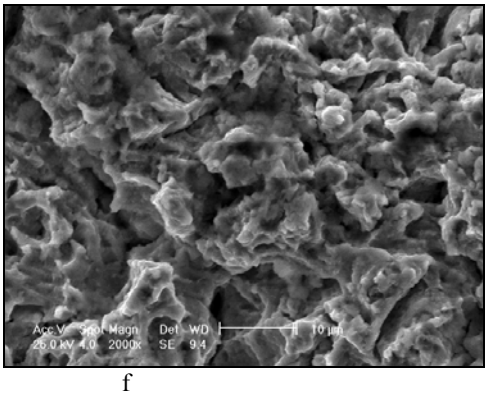

f

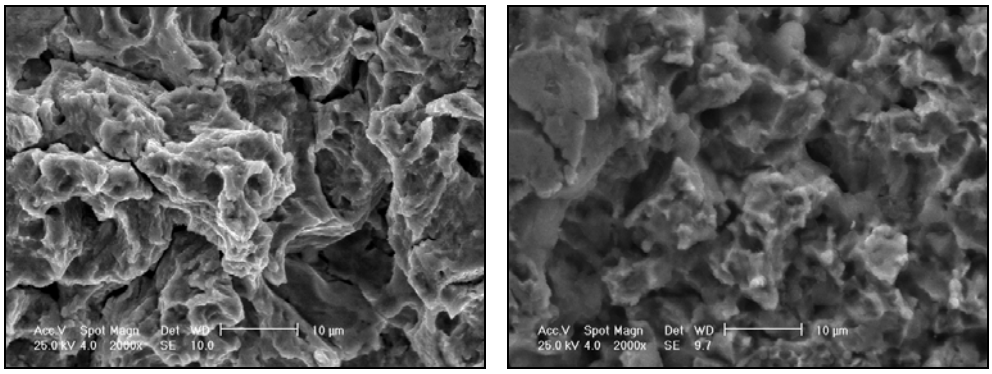

g h

Fig. 4. Structural analysis at scanning electron microscope (SEM),
after 165 minutes of cavitation loading (x2000):
a- steel A, b- steel B, c- steel C, d-steel D,
e- steel E, f-steel F, g-steel G, h- steel H

The spectrometer of the each stainless steel XRD (Fig. 5) was compared with the ICDD records and it was found that they correspond.

Also, the X-ray diffraction analysis shows the evolution of the X-ray beam intensity, depending on the diffraction angle of each stainless steel investigated. For stainless steel A was identified austenite (γ) alloyed with chromium and nickel and ferrite (α) alloyed with 36% nickel, with faced-centered cubic structure (Fig. 5a). At, steel B was identified ferrite (α) alloyed with nickel and silicon and austenite (γ) alloyed with chromium and nickel, with indicating the diffraction planes (Fig. 5b). Also, in Fig. 5c, which is from steel C is presented austenite (γ) alloyed with nickel and silicon who have crystal system faced-centered cubic and hexagonal. At, steel D from Fig. 5d, was identified the existing of austenite (γ) highlighting the alloying elements and the structure of this is faced-centered cubic and monoclinic.

In stainless steel E was identified ferrite (α) alloyed with nickel and austenite (γ) alloyed with type chromium and nickel with the primitive cubic structure and faced-centered cubic (Fig. 5e). On Fig. 5f, XRD stainless steel F, containing ferrite (α) alloyed complex with highlighting the alloying elements and austenite (γ) alloyed with chromium and nickel , where the structure are faced – centered cubic.

In XRD of stainless steel G one may remark ferrite (α) alloyed with chromium and austenite (γ) alloyed with chromium and nickel, in comparison with steel H, which contains austenite (γ) alloyed with nickel and chromium and ferrite (α) with nickel and ferrite (δ) alloyed with aluminum and nickel.

In the analyzed stainless steels, for the stainless steel H beside the presence of ferrite (α) and austenite (γ), that is found in the other stainless steels, one can notice the presence of ferrite (δ).

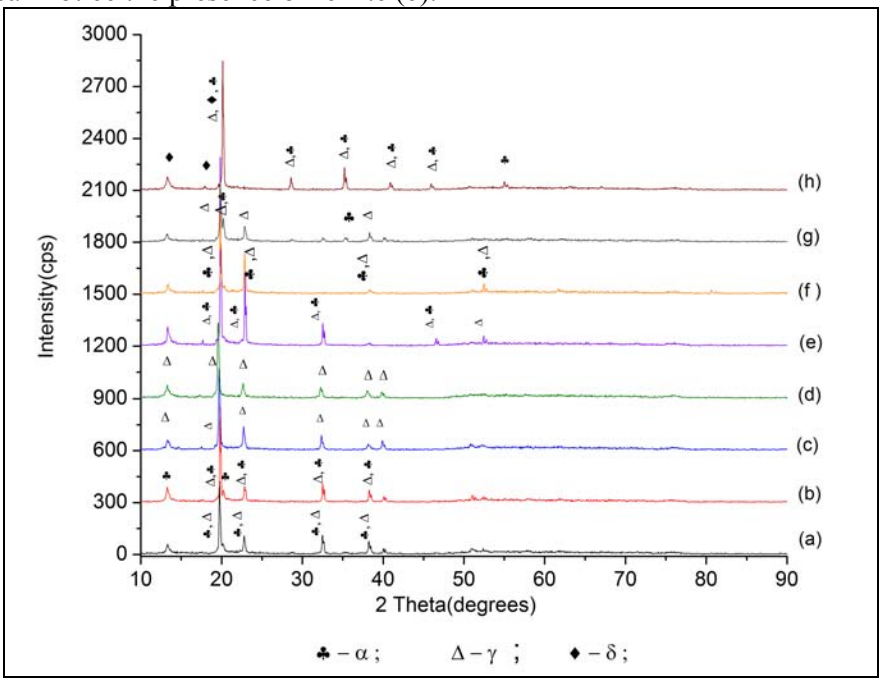

Fig. 5 XRD of experimental stainless steel:
a- steel A, b- steel B, c- steel C, d-steel D, e- steel E, f-steel F, g-steel G, h- steel H

4. Conclusions

The experiments of cavitation phenomena made on different stainless steels may reveal the following conclusions:

- The SEM analysis reveals different aspects of the affected surface through corrosion were found: very fine cavitations; many cavity uniform degradation with fine and intergranulation very fine cracks and dimensions of cavitations about 10-15μm; surface with equal proportions of fine and big cavitations, with secondary intergranular cracks and cleavage planes.
- The quantitative aspects of cavitation may decrease the cavitation resistance so, in samples of austenite stainless steels C the maximum depth of cavitation is 540μm higher than austenite-ferrite stainless steels B where the depth is only 275 μm. Also, the best cavitation behaviour (between our investigated stainless steels) is for austenite – ferrite stainless steel E, with about 38% surface affected by cavitation in comparison with

austenite stainless steel C where is the highest surface affected by cavitation about 43.85%. Thus, the best ferrous material that can be used in corrosive medium, from the ones presented in this paper, is austenite-ferrite stainless steel E.

- The stainless steels analyzed have 100% austenitic structures and austenite-ferrite with different percentages and precipitates of austenite and ferrite, and in stainless steel H on may observe the delta phase.
- The results confirmed the observations made with SEM method and macro structural analysis.

Future research plans, based on our results help for either the development of new materials with increased erosion cavity resistance, or in knowing the mechanism of cavitation evolution during erosion.

Acknowledgements

The work has been funded by the Sectoral Operational Programme Human Resources Development 2007-2013 of the Romanian Ministry of Labour, Family and Social Protection through the Financial Agreement POSDRU/88/1.5/S/60203.

R E F E R E N C E S

[1] *A. Philippy*, *W. Lauterbornz*, Cavitation erosion by single laser-produced bubbles*,* Cambridge University Press, United Kingdom, J. Fluid Mech. , vol. 361, pp. 75-116, 1998

[2] *John Carlton*, Cavitation Erosion Dynamics: Some Observations in Relation to Offshore Supply Ships, Offshore supply vessel conference, Singapore, august 2011

[3] *M. Szkodo*, Cavitation erosion of laser processed Fe-Cr-Mn and Fe-Cr-Co alloys, Journal of Achievements in Materials and Manufacturing Engineering, Vol 31, ISSSUE 2, december 2008

[4] *Muthukannan Duraiselvam , Rolf Galun, Volker Wesling , Barry L. Mordike , Rolf Reiter , Jörg Oligmüller*, "Cavitation erosion resistance of AISI 420 martensitic stainless steel laser-clad with nickel aluminide intermetallic composites and matrix composites with TiC reinforcement", Surface & Coatings Technology 201, 1289–1295, 2006

[5] *M-E. Mânzână, B. Ghiban, N. Ghiban, I. Bordea□u, F. Miculescu, M. Marin*, "Different Aspects Of Cavitation Damages In Some Stainless Steels", ANALELE UNIVERSITĂȚII "EFTIMIE MURGU" REȘIȚA, september, 2011

[6] *Mădălina-Elena Mânzână, Brândua Ghiban, Nicolae Ghiban, Ilare Bordea□u, Florin Miculescu, Sorina Mitrea, Mihai Marin*, Structural Analysis Of Cavitation For Different Stainless Steels, ANALELE UNIVERSITĂȚII "EFTIMIE MURGU" REȘIȚA, september, 2011

[7] *B. Ghiban, I. Bordeaşu, N. Giban, F. Miculescu, M. Marin & M-E. Manzana*, Structural aspects of cavitation for different copper alloys, Annals of DAAAM for 2010& Proceeding of the 21th International DAAAM Symposium, Volume 21, No.1, pp.0187-0188, Zadar Croatia, october 2010, DAAAM International VIENNA 2010

[8] *John Carlton*, "Marine Propellers and Propulsion", second edition, Elsevier Ltd, London, 2007
[9] ASM Handbook Metals Handbook, Corrosion, volume 13, ASM International, Printed in the United States of America, 1987
[10] *N. Ghiban , I. Bordeaşu , B. Ghiban , M.-E. Mânzână*, "Macrostructural Analysis Of Cavitantion For Various Ferrous Materials", Metalurgia international, vol.XVI, No.4, 2011, Material science research and development.
[11] *I. Bordeasu,B. Ghiban, M.O. Popoviciu, V. Balasoiu, N. Birau, A. Karabenciov*,. "The Damage of Austenite - Ferrite Stainless Steels by Cavitation Erosion", Proceeding of the 19th International Daaam Symposium " Intelligent Manufacturing & Automation, 22-25th October 2008, Trnava, Slovakia, Pg. 0147-0148
[12] *Kendrick H. Light,* Development of a cavitation erosion resistant advanced material system, The Graduate School The University of Maine, August, 2005
[13] *** Sonics & Materials, Inc., Cavitation Erosion Testing (ASTM G32-92)
[14] *F. Miculescu, I. Antoniac, L. Toma Ciocan, M. Miculescu, M. Branzei, A. Ernuteanu, D. Batalu, A. Berbecaru,* "Complex analysis on heat treated human compact bones", University Politehnica of Bucharest, Scientific Bulletin , Seria B, Chemisty and Materials Science, vol 73, Iss.4, 2011